

The gaseous QUAD pixel detector

C. Ligtenberg^a, Y. Bilevych^b, K. Desch^b, H. van der Graaf^a, M. Gruber^b, F. Hartjes^a, K. Heijhoff^{a,b}, J. Kaminski^b, P.M. Kluit^{a,*}, N. van der Kolk^a, G. Raven^a, L. Scharenberg^b, T. Schiffer^b, S. Schmidt^b, J. Timmermans^a

^aNikhef, Science Park 105, 1098 XG Amsterdam, The Netherlands

^bPhysikalisches Institut, University of Bonn, Nussallee 12, 53115 Bonn, Germany

Abstract

A gaseous pixel detector has been developed based on four Timepix3 chips that can serve as a building block for e.g. a large Time Projection Chamber readout plane. The quad was designed to have minimum electrical field inhomogeneities and distortions, achieving a tracking precision in the pixel plane with systematics of better than 20 μm . Due to the high efficiency to detect the ionization electrons a precise measurement of the energy loss dE/dx can be performed. In this article we present details about the construction of the quad and the results from a recent test beam experiment performed at the ELSA electron beam in Bonn where a silicon telescope was used to provide accurate tracking to study the quad detector.

Keywords: Micromegas, gaseous pixel detector, micro-pattern gaseous detector, Timepix, GridPix, Time Projection Chamber

1. Introduction

A GridPix detector is a CMOS pixel readout chip with a gas amplification grid added by MEMS postprocessing techniques. Since the invention of the GridPix detectors, a series of developments have taken place that culminated in GridPix detectors using the Timepix chip [1, 2, 3].

Recently, the first results of a single-chip GridPix detector based on the Timepix3 chip [4] have been analyzed and published [5]. The single-chip detector detects single ionization electrons with a granularity of 256×256 pixels with a pitch of $55 \mu\text{m}$ by $55 \mu\text{m}$. The measurement of the drift time and time over threshold allows a precise measurement of the drift position. Diffusion is found to be the dominating error on the track position measurement and systematic distortions in the pixel plane are below $10 \mu\text{m}$. Using a truncated sum, an energy loss (dE/dx) resolution of 4.1% based on electron counting is found for an effective track length of 1 m.

In a next step, covering larger detector surfaces, a quad detector consisting of four Timepix3 chips was designed in the context of a Time Projection Chamber for a future electron-positron collider. The performance of the quad was measured at the ELSA test beam facility in Bonn.

The device can be used in a Time Projection Chamber, in other particle physics experiments [6] and applied for medical imaging such as proton radiotherapy.

2. Quad detector design and construction

The technical steps of making a GridPix detector out of the Timepix3 chip are described in detail in [5]. For the quad detector the masks for making the grid and dyke structures were

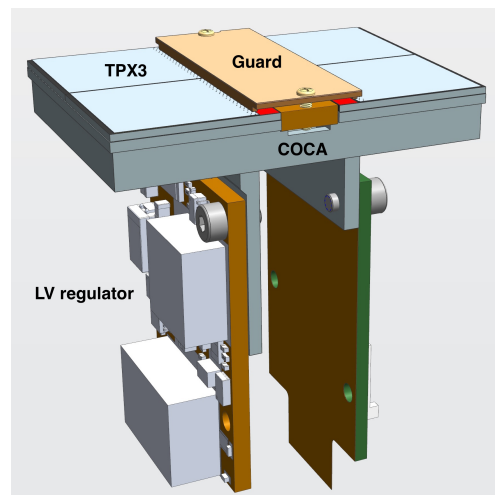


Figure 1: Schematic view of the quad detector with four Timepix3 chips mounted on the COld CARRIER plate, indicating location of the central Guard electrode and the Low Voltage Regulator.

reoptimized and a new batch of GridPixes was produced at IZM in Berlin. The quality of the new grids in terms of flatness and homogeneity is excellent. The quad was designed to maximize the sensitive detector area, keeping the electric field as homogeneous as possible while at the same time allowing for a proper cooling of the device. The material budget was kept small but can certainly be further minimized.

The quad detector shown in Figure 1, consists of a baseplate, called COCA, carrying the four Timepix3 chips and providing the cooling. The chips are electrically connected by wirebonds to a 6 mm wide PCB between the two pairs of chips. The wire-bond PCB ends at one edge into a 15 cm long Kapton cable containing the control lines and output lines of the chips that is bent downwards under the COCA. A short Kapton cable at

*Corresponding author

Email address: peter.kluit@nikhef.nl (P.M. Kluit)

the other edge of the wirebond PCB provides a low impedance 80
 45 connection to the low voltage (LV) regulator. The grids are connected to an HV filtering board. The connection to the common HV input uses a 100 M resistor for each grid to rapidly quench a micro-discharge. To support and cool the LV regulator board and the HV filtering board, a U-shaped support is attached by
 50 thermally conductive glue under the COCA. Finally, the wirebonds of the quad are covered by a 10 mm wide central guard 85
 electrode located 1.1 mm above the grids to maintain a linear drift field.

In the present design, the COCA and the U-shaped support
 55 are made of aluminium. The chips were mounted with a high precision of about 20 μm . The external quad dimensions are 39.6 x 28.38 mm of which 68.9% is active. 90

3. Quad test beam results

From the quad a small Time Projection Chamber with a ho-
 60 mogeneous drift field was made by adding a 40 mm high field cage. The device was enclosed in a gas tight container and tested in October 2018 at the ELSA test beam facility that provided 2.5 GeV electrons. The quad TPC was sandwiched between 2 x 3 planes of a Mimosa26 telescope, each consisting of
 65 a MAPS pixel detector with a pitch of 18.4 μm x 18.4 μm . The telescope was used to precisely measure and define the tracks. The quad was read out in the data driven mode with the SPIDR board and software [7]. The telescope hits were collected in time frames of 115.2 μs . Due to the high beam
 70 intensity of about 10kHz, the telescope frame often contained the data of more than one track. The chamber was flushed with an Ar/CF₄/iC₄H₁₀ 95/3/2 mixture. The grid voltage was set at 330 V and the drift field at 400 V/cm, the point where the drift velocity is near its maximum.

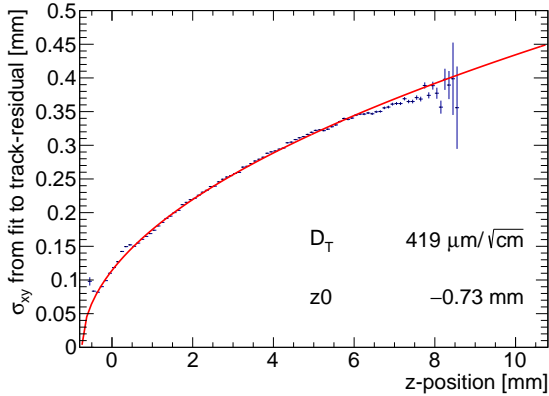


Figure 2: The single electron resolution in the transverse plane as a function of the predicted z position.

75 The data for three runs taken at different quad positions were combined to cover the full quad acceptance. A total of 400k 110
 clean tracks were selected for the results presented below. In the analysis the individual chips of the quad were carefully aligned using the tracks fitted to the silicon telescope hits.

The resolution of the single electrons in the transverse (xy) plane was measured as function of the predicted z (drift) position, as shown in Figure 2. The resolution σ_{xy} is given by:

$$\sigma_{xy}^2 = \frac{d_{\text{pixel}}^2}{12} + D_T^2(z - z_0), \quad (1)$$

where z_0 is the position of the grid and $d_{\text{pixel}}/\sqrt{12}$ was fixed to 15.9 μm . This function was fitted to the data and the transverse diffusion coefficient D_T was measured to be 419 $\mu\text{m}/\sqrt{\text{cm}}$. This value is for zero magnetic field; in a 3.5 Tesla magnetic field the diffusion is about a factor 10 smaller. For a 1 m long track one will fit about 10k single electron hits, allowing for a very accurate measurement of the track parameters.

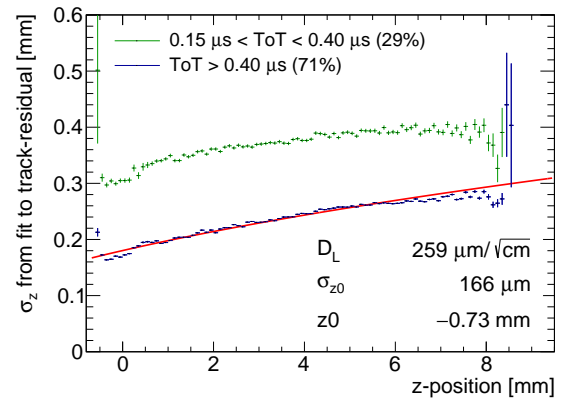


Figure 3: The single electron resolution in the longitudinal (drift) plane as a function of the predicted z position.

To extract the resolution in the drift (z) direction, the data were corrected for time slewing using the pixel by pixel time over threshold (ToT) data provided by the Timepix3 chip. The drift velocity v_{drift} was calibrated using the telescope and measured to be 54.5 $\mu\text{m}/\text{ns}$. The resolution σ_z is given by:

$$\sigma_z^2 = \frac{\tau^2 v_{\text{drift}}^2}{12} + \sigma_{z_0}^2 + D_L^2(z - z_0) \quad (2)$$

with $\tau = 1.56$ ns and σ_{z_0} is left free in the fit. The resolution, shown in Figure 3 was fitted as a function of the predicted z position from the track. The longitudinal diffusion coefficient D_L was determined to be 259 $\mu\text{m}/\sqrt{\text{cm}}$.

105 It is important to measure deformations in the xy plane. This was done by measuring the mean transverse (xy) residuals over the quad plane using the tracks defined by the telescope. It was found that a distortion was present near the edges of the chips and quad. The cause was twofold; firstly there is a geometrical bias due to the fact that at the edge of the detector only part of the ionization cloud will be detected. Secondly, a non-uniformity of the electric field was found - a grounded region - located at the edge of the dyke. A correction function based on Breit-Wigner functions is used to correct for the geometrical bias and the non-uniformity of the field. The maximum correction for the non-uniformity of the field was 150 μm . The mean transverse residuals - using bins of 4x4 pixels - over the quad

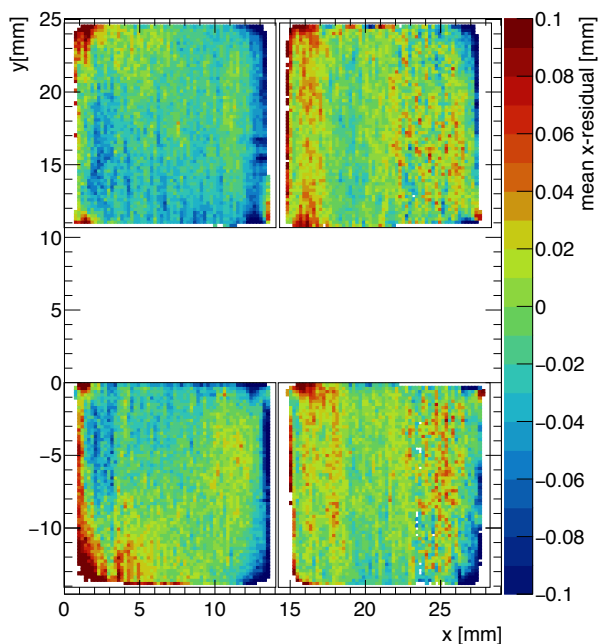


Figure 4: Average deformations in the transverse plane as a function of the predicted position in the quad xy plane.

plane after correction are shown in Figure 4. The r.m.s. of the distribution of the measured mean values over the xy surface - or the systematic error for a measurement in the xy plane - is 26 μm , without the correction it was 34 μm . It is possible that by an improved analysis of the data this value can be further reduced and brought closer to the single-chip detector performance result of 7 μm [5]. The distortions can be reduced by improving the homogeneity of the electric field near the dyke by e.g. adding a field wire to the quad detector.

4. Conclusions and Outlook

Starting with the GridPix detector using a single Timepix3 chip, a quad detector based on four chips has been designed. The detector has dimensions of 39.6 x 28.38 mm and an active surface of 68.9%. It can be used as a building block to cover large detection areas. The quad detector was operated reliably at the ELSA test beam facility. First results for the single electron resolutions in the transverse and longitudinal planes are similar to the results obtained for the single-chip detector. It has been shown that a systematic error for a measurement in the xy plane of 26 μm can be achieved.

The next step in demonstrating the potential of the GridPix technology, is the construction of a module with 2 x 4 quads. A first module has assembled and equipped with eight quads. Additional field wires have been added to improve the homogeneity of the electric field. The module can serve as a large high-resolution tracking detector with a 62 cm^2 active area.

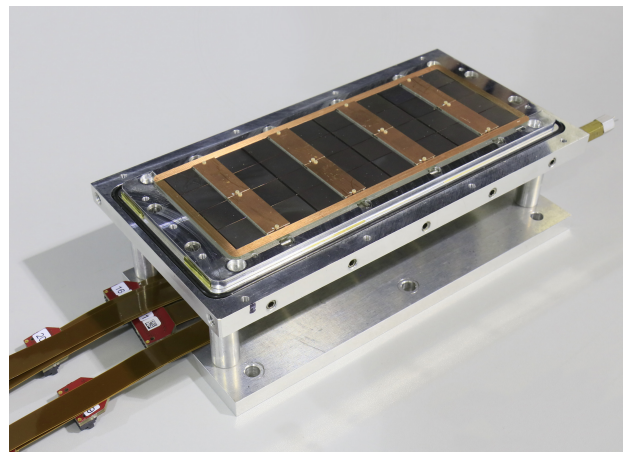


Figure 5: Photograph of the first realized module.

References

- [1] P. Colas, A. P. Colijn, A. Fornaini, Y. Giomataris, H. van der Graaf, E. H. M. Heijne, X. Llopart, J. Schmitz, J. Timmermans, J. L. Visschers, The readout of a GEM- or micromegas-equipped TPC by means of the Medipix2 CMOS sensor as direct anode, *Nucl. Instrum. Meth. A535* (2004) 506–510. doi:10.1016/j.nima.2004.07.180.
- [2] M. Campbell, et al., The Detection of single electrons by means of a micromegas-covered MediPix2 pixel CMOS readout circuit, *Nucl. Instrum. Meth. A540* (2005) 295–304. arXiv:physics/0409048, <http://dx.doi.org/10.1016/j.nima.2004.11.036> doi:10.1016/j.nima.2004.11.036.
- [3] J. Kaminski, Y. Bilevych, K. Desch, C. Krieger, M. Lupberger, GridPix detectors - introduction and applications, *Nucl. Instrum. Meth. A845* (2017) 233–235. doi:10.1016/j.nima.2016.05.134.
- [4] T. Poikela, J. Plosila, T. Westerlund, M. Campbell, M. D. Gaspari, X. Llopart, V. Gromov, R. Kluit, M. van Beuzekom, F. Zappone, V. Zivkovic, C. Brezina, K. Desch, Y. Fu, A. Kruth, Timepix3: a 65k channel hybrid pixel readout chip with simultaneous toa/tot and sparse readout, *Journal of Instrumentation* 9 (05) (2014) C05013. URL <http://stacks.iop.org/1748-0221/9/i=05/a=C05013>
- [5] C. Ligtenberg, K. Heijhoff, Y. Bilevych, K. Desch, H. van der Graaf, F. Hartjes, K. Kaminski, P. M. Kluit, G. Raven, T. Schiffer, J. Timmermans, Performance of a GridPix detector based on the Timepix3 chip, *Nucl. Instrum. Meth. A908* (2018) 18–23. doi:10.1016/j.nima.2018.08.012.
- [6] C. Krieger, J. Kaminski, M. Lupberger, K. Desch, A GridPix-based X-ray detector for the CAST experiment, *Nucl. Instrum. Meth. A867* (2017) 101–107. doi:10.1016/j.nima.2017.04.007.
- [7] J. Visser, M. van Beuzekom, H. Boterenbrood, B. van der Heijden, J. I. Muñoz, S. Kulis, B. Munneke, F. Schreuder, SPIDR: a read-out system for Medipix3 & Timepix3, *Journal of Instrumentation* 10 (12) (2015) C12028. doi:10.1088/1748-0221/10/12/C12028.